Journal of Thermal Analysis and Calorimetry, Vol. 90 (2007) 3, 795–799

CHANGES IN THE HEAT CAPACITY OF Al_2O_3–Cr_2O_3 SOLID SOLUTIONS NEAR THE POINT OF ANTIFERROMAGNETIC PHASE TRANSITION IN Cr_2O_3

V. A. Drebushchak[1,2*] *and A. I. Turkin*[1]

[1]Institute of Geology and Mineralogy, Siberian Branch of the Russian Academy of Sciences, pr. Koptyuga, 3
Novosibirsk 630090 Russia
[2]Research and Education Center ‘Molecular Design and Ecologically Safe Technologies’, REC-008, Novosibirsk State University
ul. Pirogova, 2, Novosibirsk 630090, Russia

Al_2O_3–Cr_2O_3 solid solutions with 0, 4, 7, 10 and 20 mol% of corundum were synthesized using a high-pressure/high-temperature apparatus and characterized by X-ray powder diffraction.

Calorimetric measurements were carried out using DSC-111 (Setaram). Heat capacity was measured by the enthalpy method in a temperature range of 260–340 K, near magnetic phase transition in pure Cr_2O_3 (305 K). Magnetic contribution into the heat capacity was derived and found to change irregularly with the composition.

Heat capacity of solid solutions remains constant in a relatively wide range of composition, while the C_p values of the end members differ significantly. This phenomenon is very important for the modeling of the thermodynamic functions of intermediate solid solutions.

Keywords: *corundum, eskolaite, heat capacity, magnetic contribution, solid solutions*

Introduction

Corundum (α-Al_2O_3) is the reference material for calorimetry (SRM720) [1] and X-ray diffraction (SRM674a and SRM1976) [2]. Its heat capacity has no anomalies over the whole temperature range up to the melting point.

Escolaite (Cr_2O_3) is isostructural with corundum, but antiferromagnetic below 305 K and paramagnetic above. Its heat capacity was investigated several times [3, 4], but the thermodynamic functions are not quite accurate because of possible impurities that appear during the decomposition of Cr_2O_3 near the melting point.

Corundum with an impurity of Cr_2O_3 (a few mol%) is known as ruby. Synthetic solid solutions of Al_2O_3 with elevated content of Cr_2O_3 are unstable at low temperatures and decay if exposed to hydrothermal treatment, but the kinetics of the decay is too slow under normal conditions, and the quenched homogeneous samples are considered ideal solid solutions [5]. In thermodynamic evaluations of the solid solutions, magnetic interaction in Cr_2O_3 is not considered at all [6].

Solid solutions of isostructural end-member phases are characterized by the relationship between structure and composition. The difference between the experimental unit cell parameters and theoretical linear function (Vegard’s rule) is considered most informative and useful in the development of Cr_2O_3–Al_2O_3 refractories [7]. Recently, we showed that the heat capacity is more effective tool for the investigation of the solid solutions of two magnetic phases (FeS and NiS) than the X-ray powder diffraction [8]. Fe–Ni monosulfide solid solutions are very unstable, with high cationic mobility, capable of decaying into two separate phases near room temperature [9]. For natural pyrrhotites, it was recognized many years ago [10]. It is very interesting to investigate how the heat capacity changes in metastable magnetic solid solutions, not decaying at heating.

The objective of this work was to measure the heat capacity of Al_2O_3–Cr_2O_3 solid solutions near the magnetic transition point of pure Cr_2O_3 and clarify how the thermodynamic functions of solid solutions change with the composition.

Experimental

Sample preparation

Chemicals Cr_2O_3, fine green powder, and Al_2O_3, fine white powder, of ‘high purity’ grade were used as starting materials. Charges for the synthesis of solid solutions were prepared from the mixtures of the ox-

---

[*] Author for correspondence: dva@uiggm.nsc.ru

1388–6150/$20.00

Akadémiai Kiadó, Budapest, Hungary
Springer, Dordrecht, The Netherlands

Table 1 Data on the solid solutions

No.	Synthesis		Sample composition			Unit cell parameter		DSC	
	Al_2O_3/ mg	Cr_2O_3/ mg	Al_2O_3/ mol%	Cr_2O_3/ mol%	formula mass/ g mol^{-1}	*a*/ nm	*c*/ nm	sample mass/ mg	No. of runs
1			–	100	151.99			505.9	6
2	–	1000	–	100	151.99	0.4947(3)	1.3544(10)	679.0	4
3	27.05	973.20	3.98	96.02	150.00	0.4945(3)	1.3545(12)	521.2	4
4	48.20	951.55	7.02	92.98	148.48	0.4936(13)	1.3523(53)	552.0	5
5	68.70	931.75	9.90	90.10	147.04	0.4928(13)	1.3532(55)	709.9	5
6	144.50	856.60	20.09	79.91	141.94	0.4911(3)	1.3487(11)	539.6	6
7			100	–	101.96			539.1	6

ides, ground and mixed under alcohol in a hard-alloy mortar. Prior to the grinding, the reagents were heated at 200°C for 3 h. Total mass of a charge was taken to be close to 1 g. The mixtures are listed in Table 1.

For the synthesis of the solid solutions, the 'split-sphere' type high-pressure/high-temperature apparatus was used. The apparatus and the synthesis was described elsewhere [11]. The synthesis was carried out at 1800–2000°C and 5–10 kbar for 6 h (1.5 h for pure Cr_2O_3). Synthesized samples were taken from a crucible and heated again at 800°C for 4 h to remove the traces of graphite, lining the internal surface of the crucibles. Synthesized solid solutions were black homogeneous tablets of 3 mm thick and 9 mm in diameter. For the heat capacity measurements, the tablets were broken down, because the internal diameter of a standard Al crucible for DSC-111 is 6 mm. The tablet of pure Cr_2O_3 was green, fragile, with faces of single crystals on the surface of the tablet. It was readily broken into single crystals up to 2 mm in size.

Methods

X-ray powder diffraction

Solid solutions were analyzed by X-ray powder diffraction using D-8 Discover diffractometer with GADDS (Bruker), CuK_α radiation. Unit cell parameters are listed in Table 1. They were refined on 5 or 6 reflections using program complex ULM [12].

Calorimetric measurements

Heat capacity was measured using DSC-111 (Setaram) in the standard Al crucible of 0.8 mm^3. Calibration of the sensitivity was performed using the corundum reference sample (COTC-1a). It was also used as the end member of the Al_2O_3–Cr_2O_3 solid solution (sample 7 in Table 1).

The measurements were carried out near the magnetic phase transition point of pure Cr_2O_3 in a temperature range of 260–340 K. The enthalpy mode was used with 200 s heating and 400 s isothermal segments. At a heating rate of 90 K h^{-1} the temperature increment was of 5 K. Sample masses of solid solutions are in Table 1. Every sample was measured several times, listed in Table 1 in the 'N of runs' column. Each time the sample was inserted into the DSC cell before a run, measured only one time, and taken off after the end of the run. Empty crucible was measured only one run, because the integral signal was found to be very small as compared with the uncertainty of the integral signal of the crucible with a sample.

Scanning heating experiments were carried out with the same samples at a heating rate of 0.2 K min^{-1}.

Results and discussion

Average values of heat capacity of the samples and the standard deviations (*s*) are listed in Table 2. The calibration coefficient was derived from the smoothed values of Al_2O_3 fitted to a polynomial, and the experimental points for this end member phase in the table also contain random errors.

Heat capacity measured by the enthalpy method is averaged over the temperature range of T_1 to T_2 of increment $\Delta T = T_2 - T_1$:

$$\overline{C}_p = \frac{\Delta H}{\Delta T}$$

These values are more precise as compared with the results of the scanning heating [13], but the averaging corrupts the shape of the peak of a phase transition. Magnetic phase transition in the recrystallized Cr_2O_3 is shown in Fig. 1. The results of both methods, scanning heating and enthalpy increment, agree well with one another, but the peak is much close to its true shape for scanning heating than for enthalpy method. For the solid solutions, the sharp peak disappears, becoming smooth and rounded. Similar difference is between the initial and recrystallized Cr_2O_3. The peak of the mag-

Table 2 Heat capacity of solid solutions with different Al_2O_3 content (J mol^{-1} K^{-1})

T/K	Initial Cr_2O_3		0%		3.98%		7.02%		9.90%		20.09%		100%	
	C_p	s	C_p	s	C_p	s	C_p	s	C_p	s	C_p	s	C_p	s
262.5	99.1	0.5	103.4	0.8	103.2	0.6	103.7	1.5	100.9	0.7	90.5	0.5	70.52	0.7
267.5	101.1	0.5	105.6	0.4	105.9	0.5	105.3	0.7	103.0	0.7	91.0	0.4	71.25	0.5
272.5	104.3	0.2	108.3	0.8	108.2	0.2	108.3	0.3	106.1	0.6	92.2	0.3	73.08	0.2
277.5	105.5	0.2	110.1	0.9	110.3	0.1	110.7	0.2	107.1	0.4	92.1	0.1	74.30	0.2
282.5	108.2	0.5	112.7	0.6	112.8	0.2	113.5	0.3	108.0	0.4	92.8	0.1	75.54	0.4
287.5	110.3	0.2	114.9	0.6	115.5	0.5	112.5	0.3	106.3	0.3	93.4	0.2	76.31	0.3
292.5	113.8	0.5	117.4	0.6	117.3	0.3	108.0	0.3	103.9	0.3	94.1	0.2	77.42	0.3
297.5	117.3	0.4	120.6	0.7	116.5	0.5	105.9	0.4	102.5	0.2	94.8	0.2	78.45	0.2
302.5	122.8	0.5	126.1	0.5	113.9	0.1	106.0	0.4	102.7	0.3	96.1	0.2	79.99	0.2
307.5	123.2	0.6	125.3	0.3	110.8	0.2	105.1	0.4	102.7	0.3	96.8	0.2	81.24	0.1
312.5	111.2	0.7	113.3	0.4	107.8	0.1	104.6	0.4	102.5	0.5	96.9	0.3	82.23	0.2
317.5	108.0	0.7	110.3	0.6	106.7	0.5	104.1	0.5	102.3	0.5	96.9	0.2	82.83	0.1
322.5	106.6	0.3	109.1	0.3	106.3	0.1	104.0	0.1	102.6	0.3	97.3	0.6	83.73	0.3
327.5	105.9	0.2	108.4	0.6	106.2	0.1	104.2	0.3	102.9	0.3	97.7	0.7	84.59	0.4
332.5	105.9	0.4	108.4	0.6	106.7	0.5	104.9	0.2	103.6	0.3	98.7	0.3	86.10	0.2
337.5	105.3	0.2	108.2	0.4	106.5	0.2	104.9	0.2	103.7	0.3	98.9	0.5	86.81	0.3

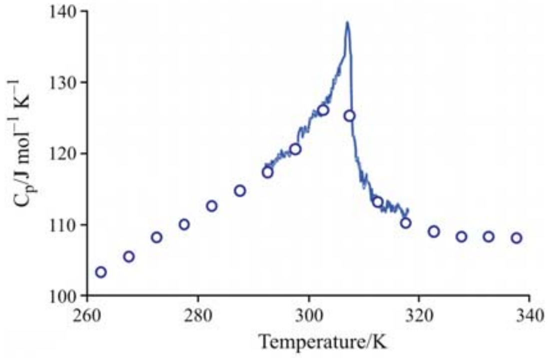

Fig. 1 Magnetic phase transition in pure Cr_2O_3 (sample 2). Recrystallized sample was measured by — – scanning heating and ○ – enthalpy method

netic phase transition is not as sharp for the fine powder of starting material as for the single crystals in the tablet. The shape of the peak is not considered in this work in detail, but the evident difference between starting powder and recrystallized sample allows us to prefer the results of the recrystallized sample.

It is evident from Table 2 that two pure samples of Cr_2O_3, the initial reagent (N1) and the recrystallized tablet (N2), differ reliably in heat capacity. It is the manifestation of a general problem in thermodynamics of magnetic phases. In literature, heat capacity values for pure Cr_2O_3 vary significantly (up to tens per cent near 298.15 K), indicating the differences in the samples investigated. There are two main reasons for the irreproducibility in C_p near the magnetic phase transition of Cr_2O_3: (*i*) the irreproducibility in the sample composition and (*ii*) irreproducibility in the sample shape and size. Cr_2O_3, melts at very high temperature (2705±30 K) with decomposition, and the samples synthesized from the melt are nonstoichiometric, with the impurity of Cr_3O_4 [14]. In turn, the parameters of the magnetic phase transition in a pure substance differ significantly for single crystals, fine powders, and thin films. Magnetization was shown to depend on the particle's size in [15] and the magnetic contribution in the heat capacity in [16]. Our results for the initial reagent and recrystallized tablet conform to the general rule that the heat capacity in the vicinity of a magnetic phase transition of a bulk sample is greater than that for fine powder. As for the comparison with literature data, C_p values for sample N2 are less than the data published in [4] but very close to those from [17], considered most reliable in the thermodynamic database [3].

End member phases of the Al_2O_3–Cr_2O_3 solid solutions differ in magnetic properties. Antiferromagnetic below 305 K, Cr_2O_3 contains a magnetic contribution (C_m) in its heat capacity:

$$C_p=C_l+C_m$$

Contrary, heat capacity of corundum is defined only by thermal vibrations in its crystalline lattice (C_l). The magnetic contribution is estimated usually as the difference in the heat capacities between magnetic and nonmagnetic isostructural phases. In applying this to our samples, we subtracted C_p of pure Al_2O_3 from those of Cr-rich solid solutions. The results are shown in Fig. 2.

Magnetic contribution turned out to be large enough as compared to the lattice contribution, as much as 50% of the latter. Sharp peak near 305 K for

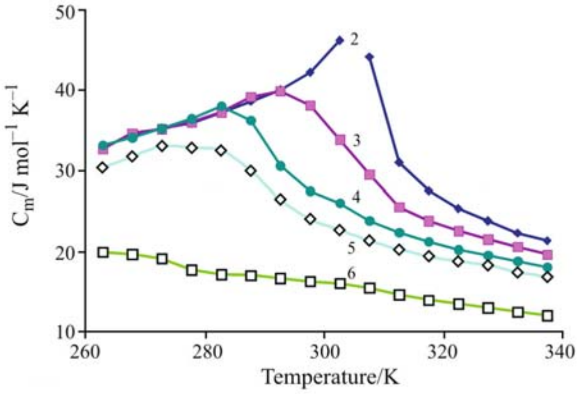

Fig. 2 Magnetic contribution to the heat capacity of Al_2O_3–Cr_2O_3 solid solutions. Numerals are the numbers of samples in Table 1

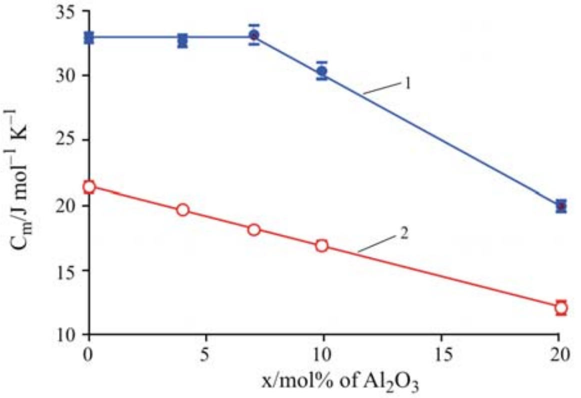

Fig. 3 Magnetic contribution as a function of the composition: 1 – before and 2 – after the phase transition

pure Cr_2O_3 becomes smoothed and reduced for solid solutions with increasing impurity of Al_2O_3. The temperature of the magnetic phase transition also decreases as the corundum content of the solid solutions increases. The values of C_m behave differently before and after the phase transition. These are shown in detail in Fig. 3.

Before the phase transition, the magnetic contribution remains nearly constant up to 7 mol% of Al_2O_3. The standard deviation of the heat capacity for the lowest temperature (262.5 K) has the greatest value among all experimental points, and we show the next point, C_p (267.5), on Fig. 3. Within the limits of experimental error, three Cr-rich solid solutions (0, 4 and 7% of Al_2O_3) have equal magnetic heat capacities. This fact is very interesting and not quite understandable, because Al^{3+} cations cannot participate in magnetic interaction by their nature. Electronic shells of Al^{3+} are similar to those of Ne. It is difficult to suppose how such cation Al^{3+} participates in the magnetic interaction between cations Cr^{3+}, producing additional contribution into the heat capacity of the solid solutions. Starting from 10 mol%, the magnetic heat capacity decreases. Extrapolation to zero value of the magnetic contribution yields the point of about 40 mol% of Al_2O_3, where the contribution disappears. Below this limit composition, cations Cr^{3+} and Al^{3+} in the solid solutions produce identical heat capacity.

After the phase transition, the magnetic contribution decreases linearly with the increase of the corundum content. Experimental points fit well to the straight line on Fig. 3. It is well understandable and even predictable, because Al^{3+} cations do not participate in the magnetic interaction and do not contribute to the magnetic heat capacity. The straight line intersects x-axis at 46 mol% of Al_2O_3, close to the value derived from the extrapolation of magnetic contribution before the phase transition.

Nearly constant heat capacity of the solid solutions near both end members is in agreement with the similar phenomenon found recently for the heat capacity of monosulfide solid solutions. C_p values were nearly constant at both end members of the $Fe_{0.96-x}Ni_xS$ solid solutions with an irregularity in between [8]. Probably, this phenomenon is general for magnetic solid solutions.

Conclusions

Cr-rich solid solutions of the Al_2O_3–Cr_2O_3 series were synthesized using sintering technique in a high-pressure/high-temperature apparatus. DSC measurements showed that the magnetic contribution to the heat capacity changes irregularly with the composition. Besides, there is a difference in the changes before and after magnetic phase transition. Ideal solution model is not applicable for the evaluation of thermodynamic properties for these solid solutions. Measured values of the heat capacity will allow us to develop the algorithm of evaluation of heat capacity, enthalpy and entropy for the Al_2O_3–Cr_2O_3 series as functions of their composition.

It was found that the heat capacity of the end member phases is constant within the limits of experimental errors in the range of composition from 0 to 7 mol% of corundum. One can also expect that the values of C_p will be constant for the Al_2O_3–Cr_2O_3 solid solutions with 50–100 mol% of corundum. Together with similar observations in monosulfide solid solutions (0–60 and 90–100 mol% of Ni), this phenomenon can be considered general for magnetic solid solutions.

This hypothesis should be checked for other solid solutions, for it is very important for the evaluation of thermodynamic functions of intermediate solid solutions. So far, the thermodynamic functions were usually derived from the models of mixing in a form of smooth functions of the composition.

Acknowledgements

The research described in this publication was made possible in part by Award No. NO-008-X1 of the U.S. Civilian Research and Development Foundation for the Independent States of the Former Soviet Union (CRDF). The work was supported by RFBR grants 05-05-64556a and 06-05-65114.

References

1 D. G. Archer, J. Phys. Chem. Ref. Data, 22 (1993) 1441.
2 M. Oetzel and G. Heger, J. Appl. Cryst., 32 (1999) 799.
3 Thermodynamic Properties of Individual Substances, V. P. Glushko, Ed., Vol. IV, Nauka, Moscow 1982 (in Russian).
4 S. Klemme, H. St. C. O'Neill, W. Schnelle and E. Gmelin, Am. Mineral., 85 (2000) 1686.
5 A. R. West, Solid State Chemistry and its Applications, John Wiley & Sons, Chichester–New York 1984.
6 N. D. Chatterjee, H. Leistner, L. Terhart, K. Abraham and R. Klaska, Am. Mineral., 67 (1982) 725.
7 O. N. Popov, V. P. Frolova, V. P. Martynov and V. Ya. Dzyuzer, Glass Ceramics, 46 (1989) 191.
8 V. A. Drebushchak and E. F. Sinyakova, J. Therm. Anal. Cal., OnlineFirst, DOI: 10.1007/s10973-006-7501-x.
9 V. A. Drebushchak, Zh. N. Fedorova and E. F. Sinyakova, J. Thermal Anal., 48 (1997) 727.
10 R. G. Arnold, Econ. Geol., 64 (1969) 405.
11 A. I. Turkin, V. A. Drebushchak and S. N. Gusak, Mater. Res. Bull., 37 (2002) 1117.
12 R. Brueggemann, B. Mueller, T. Debaerdemaeker, G. Schmid and U. Thewalt, Computing Program Complex ULM for X-ray Crystallography, University of Ulm, Germany 1992.
13 T. Mitsuhashi and A. Watanabe, J. Therm. Anal. Cal., 60 (2000) 683.
14 H. Wartenberg and K. Eckhardt, Z. Anorg. Allg. Chem., 232 (1937) 179.
15 Y. Ichiyanagi, T. Uehashi, S. Yamada, Y. Kanazawa and T. Yamada, J. Therm. Anal. Cal., 81 (2005) 541.
16 Y Miyazaki, T. Sakakibara, H. Miyasaka, N. Matsumoto and M Sorai, J. Therm. Anal. Cal., 81 (2005) 603.
17 C. T. Anderson, J. Am. Chem. Soc., 59 (1937) 488.

Received: November 20, 2006
Accepted: January 17, 2007
OnlineFirst: April 29, 2007

DOI: 10.1007/s10973-006-8271-1